Heliyon 6 (2020) e03831

Contents lists available at ScienceDirect

Heliyon

journal homepage: www.cell.com/heliyon

Research article

Formulating octyl methoxycinnamate in hybrid lipid-silica nanoparticles: An innovative approach for UV skin protection

T. Andreani [a,b], J. Dias-Ferreira [c], J.F. Fangueiro [c], A.L.R. Souza [d], C.P. Kiill [d], M.P.D. Gremião [d], M.L. García [e,f], A.M. Silva [a,b], E.B. Souto [c,g,*]

[a] Department of Biology and Environment, University of Tras-os-Montes e Alto Douro, UTAD, Quinta de Prados, P-5001-801 Vila Real, Portugal
[b] Centre for Research and Technology of Agro-Environmental and Biological Sciences (CITAB-UTAD), Quinta de Prados, 5001-801 Vila Real, Portugal
[c] Faculty of Pharmacy, University of Coimbra, Pólo das Ciências da Saúde, Azinhaga de Santa Comba, 3000-548 Coimbra, Portugal
[d] School of Pharmaceutical Sciences, UNESP – Universidade Estadual Paulista, Rodovia Araraquara-Jau Km 1, Araraquara, SP 14801-902, Brazil
[e] Department of Physical Chemistry, Faculty of Pharmacy, University of Barcelona, Av. Joan XXIII s/n, 08028 Barcelona, Spain
[f] Institute of Nanoscience and Nanotechnology, University of Barcelona, Av. Joan XXIII s/n, 08028 Barcelona, Spain
[g] CEB – Centre of Biological Engineering, University of Minho, Campus de Gualtar, 4710-057 Braga, Portugal

ARTICLE INFO

Keywords:
Pharmaceutical science
Pharmaceutical chemistry
Nanotechnology
Octyl methoxycinnamate
Solid lipid nanoparticles
SLN
Silica hybrid nanoparticles
Sunscreens
Hydrogel

ABSTRACT

Sunscreens have been employed on daily skin care for centuries. Their role in protecting the skin from sun damage, avoiding accelerated photoaging and even limiting the risk of development of skin cancer is unquestionable. Although several chemical and physical filters are approved as sunscreens for human use, their safety profile is dependent on their concentration in the formulation which governs their acceptance by the regulatory agencies. A strategic delivery of such molecules should provide a UV protection and limit the skin penetration. Solid lipid nanoparticles (SLN) and nanostructured lipid carriers (NLC) may offer an alternative approach to achieve a synergistic effect on the UV protection when loaded with sunscreens as particles themselves also have a UV light scattering effect. Besides, the lipid character of SLN and NLC improves the encapsulation of lipophilic compounds, with enhanced loading capacity. Silica nanoparticles have also been employed in sunscreen formulations. Due to the formed sol-gel complexes, which covalently entrap sunscreen molecules, a controlled release is also achieved. In the present work, we have developed a new sunscreen formulation composed of hybrid SLN-Silica particles loaded with octyl methoxycinnamate (Parsol®MCX), and their further incorporation into a hydrogel for skin administration. Hybrid SLN-silica particles of 210.0 ± 3.341 nm of mean size, polydispersity below 0.3, zeta potential of ca. |7| mV, loading capacity of 19.9% and encapsulation efficiency of 98.3% have been produced. Despite the slight negative surface charge, the developed hybrid nanoparticles remained physicochemically stable over the study period. Turbiscan transmission profiles confirmed the colloidal stability of the formulations under stress conditions. The texture profile analysis of Parsol-SLN and Parsol-SLN-Si revealed semi-solid properties (e.g. adhesiveness, hardness, cohesiveness, springiness, gumminess, chewiness, resilience) suitable for topical application, together with the bioadhesiveness in the skin of pig ears. The non-irritation profile of the hybrid nanoparticles before and after dispersion into Carbopol hydrogels was confirmed by HET-CAM test.

1. Introduction

Sunscreens or UV blockers are commonly used to minimize sunburns, which are responsible for an early onset of skin aging and even for the enhanced risk of both melanoma and non-melanoma skin cancer [1]. Sunscreens are mainly classified in two categories – organic versus inorganic sunscreens. The former comprise molecules as salicylates which absorb the UV radiation in a relatively narrow wavelength when directly applied onto the skin [2]. These molecules undergo a relatively fast photodegradation thereby showing short lifetime, frequently causing allergic reactions and may even be absorbed by the skin [3, 4]. Inorganic sunscreens (e.g. titanium dioxide, zinc oxide) exhibit a wider UV absorption band as they combine absorption and scattering of UVA and UVB radiations. A synergistic (or at least an additive) effect may be obtained when combining organic and inorganic UV blockers in a topical formulation. Another approach to improve the performance of both types

* Corresponding author.
E-mail addresses: ebsouto@ff.uc.pt, souto.eliana@gmail.com (E.B. Souto).

https://doi.org/10.1016/j.heliyon.2020.e03831
Received 20 October 2018; Received in revised form 24 January 2020; Accepted 20 April 2020

of sunscreens is their loading into nanoparticles of varied nature e.g. solid lipid nanoparticles (SLN) [5, 6, 7], silica nanoparticles (Si-NPs) [8, 9], as nanoparticles also have light scattering capacity [6]. SLN are composed of biodegradable and biocompatible lipids (e.g. triglycerides, fatty acids, waxes) [10], whereas Si-NPs result from the co-condensation of organotrialkoxysilane monomer and silica monomer (e.g. TEOS, tetraethoxysilane), using ethanol in ammonia as the organic solvent to obtain Si-NPs in suspension [11, 12]. Depending on the lipophilic character of the sunscreen, a high loading capacity can be achieved either by physical encapsulation within the nanoparticle matrix or by chemical covalent bonding. Hydrophobic sunscreen molecules can be easily loaded within the lipid core of SLN or formulated in oil/water (o/w) polymerized microemulsions during the production of silica particles. Hydrophilic sunscreens can be incorporated through a reverse water/oil (w/o) microemulsion process [13, 14].

Parsol® MCX (2-ethylhexyl 4-methoxycinnamate or octyl methoxycinnamate) is a water-resistant, colorless UVB filter, frequently found in combination with other sunscreens. It is easily formulated in the lipid phase of cosmetic products, being thereby a good candidate for the loading into nanoparticles. To circumvent the use of organic solvents, we propose a new type of nanoparticles – hybrid nanoparticles – composed of lipids and silica, to be loaded with octyl methoxycinnamate (Parsol® MCX). For topical application, a semi-solid hydrogel formulation has also been developed with a gel forming agent (Carbopol® 971); the irritation profile of particles before and after dispersion into hydrogels has been analysed by HET-CAM test.

2. Materials and methods

2.1. Materials

Parsol® MCX (2-ethylhexyl 4-methoxycinnamate or octyl methoxycinnamate) was purchased from Acofarma (Barcelona, Spain). Tetraethyl orthosilicate (TEOS, 98%) was purchased from Merck (Darmstad, Germany). Cetyl palmitate (solid lipid) was purchased from Sigma-Aldrich (Portugal). Tego Care® 450 (surfactant) was obtained from Evonik Industries (Germany). Carbopol® 971P NF Polymer was purchased from Lubrizol (Wickliffe, USA). MilliQ Plus system (Millipore, Germany) was used as source of water of high purity used in the study.

2.2. Preparation of blank-SLN and Parsol-SLN

High shear homogenization method was used for the production of SLN (blank-SLN) [15]. Particles were composed of cetyl palmitate (solid lipid) stabilized with polyglyceryl-3 methylglucose distearate (Tego Care®450) as surfactant. Briefly, cetyl palmitate was melted in a beaker heated at 65 °C. The aqueous phase, composed of water and Tego Care®450, was heated up to the same temperature. Both phases were mixed together under stirring at 10 000 rpm, using an Ultra-Turrax T25 for 15 min. The dispersions were cooled down under ice bath for 10 min, allowing the lipid to recrystallize and generate blank-SLN. For the Parsol® MCX loaded hybrid nanoparticles (Parsol-SLN), Parsol® and TEOS were added to the melted cetyl palmitate prior to the hot shear emulsification, following the same process as described for blank-SLN. Table 1 lists the composition and concentration for each developed formulation.

2.3. Quantification of encapsulation parameters

The encapsulation parameters, i.e. encapsulation efficiency (EE) and loading capacity (LC), of octyl methoxycinnamate (OMC, Parsol® MCX) loaded within cetyl palmitate-SLN were determined applying the follow equations:

$$EE\% = \frac{W_{OMC} - W_s}{W_{OMC}} \times 100 \quad (1)$$

$$LC\% = \frac{W_{OMC} - W_s}{W_{OMC} - W_s + W_L} \times 100 \quad (2)$$

where W_{OMC} is the mass of octyl methoxycinnamate (OMC, Parsol® MCX) weighted to prepare SLN, W_L is the mass of cetyl palmitate weighted to prepare SLN, and W_s is the mass of octyl methoxycinnamate quantified at 310 nm in the supernatant. Briefly, a volume of Parsol-SLN was ultracentrifuged for 1 h at 100,000 $\times g$ in a ultracentrifuge (Beckman Optima™ XL, Indianapolis, USA), after which OMC was quantified in the supernatant in a UV spectrophotometer (Shimadzu UV-1601, Shimadzu, Cornaredo, Italy).

2.4. Incorporation of Parsol-loaded hybrid nanoparticles in hydrogels

Hybrid nanoparticles were incorporated in hydrogels to achieve suitable viscosity for topical application. The preparation of hydrogels consisted in the addition of 1.0% (w/v) of the gel forming agent (Carbopol® 971) to 99% of distilled water under gentle magnetic stirring at 300 rpm. Then, the aqueous dispersion was neutralized using a NaOH solution (10.0%) to reach the pH of 7.0. SLN formulations were incorporated into hydrogels adding 20.0 mL of SLN dispersions to 10.0 g of Carbopol hydrogels followed by high speed stirrer (Cito-Unguator, Gaco International, UK) for 1 min, followed by 30 s in the ultrasound bath for the eventual removal of air bubbles.

2.5. Particle size analysis and zeta potential (ZP) measurements

Dynamic light scattering (DLS, Zetasizer Nano ZS, Malvern Instruments, Malvern, UK) was used to characterize SLN dispersions with respect to the mean particle size, polydispersity index (PI) and zeta potential (ZP). For the determination of the mean particle size and PI, each dispersion was diluted in ultra-purified water at a ratio that avoids particle scattering (1:100) and the mean size and PI were assessed at a fixed angle of 173°. Measurements were done at the temperature of 25 °C. For ZP analysis, nanoparticles were also diluted at the same ratio (1:100) with purified water of conductivity adjusted to 50 $\mu S.cm^{-1}$ by adding 0.9% NaCl solution. ZP was measured by laser Doppler electrophoresis at 25 °C. Size parameters and ZP were recorded at pre-determined time intervals (day 0, and 7, 15 and 30 days after production). Each recorded value was obtained from the average of three measurements (each measurement results from the average of 10 runs).

2.6. Long-term physical stability of hybrid nanoparticles by TurbiscanLab® analysis

The physical stability of SLN dispersions was monitored using an optical analyser TurbiscanLab® (Formulaction, France), composed of a near-infrared light source (880 nm), and two synchronous transmission (T) and backscattering (BS) detectors. Experiments were conducted at 25 °C. The SLN dispersions were placed in a cylindrical glass cell. The T detector received the light crossing SLN dispersions, while the BS

Table 1. Composition of the developed formulations (w/w %).

Components	Blank SLN	Parsol-SLN	Parsol-SLN-Si
Cetyl palmitate	5.0	4.0	4.0
Tego Care® 450	1.0	1.0	1.0
TEOS	-	-	1.0
Parsol	-	1.0	1.0
Water	84.0	84.0	83.0

Si: Silica coating.

detector received the light scattered backwards. T and BS were recorded each 40 μm, 3 times over a period of 10 min, from the scanning of the entire height of the sample by the detection head.

2.7. Differential scanning calorimetry (DSC)

A Mettler DSC 823e (Mettler Toledo, Spain) was used for the DSC measurements. Prior to analysis, indium of purity ≥99.95% (Fluka, Switzerland) was used to calibrate the device. Accurately weighted mass of 1.0–2.0 mg of cetyl palmitate, octyl methoxycinnamate (Parsol® MCX), or an equivalent amount of lipid formulated as hybrid nanoparticles, were weighted in aluminium pan of 40.0 μl, which were then cold sealed. An empty pan was used as reference. Heating curves for the bulk materials were recorded with a scan rate of 5.0ºC/min from 25.0 to 200.0 °C and then cooled down to 25.0 °C, using liquid nitrogen. For the analysis of SLN formulations, heating curves were recorded from 25.0 °C to 85.0 °C following cooling down to 25.0 °C, at a scan rate of 5.0ºC/min. The Mettler STARe V 9.01 DB software (Mettler Toledo, Spain) was used for the collection and storage of the data of peak areas.

2.8. Bioadhesion analysis of hybrid nanoparticles and hydrogels

The Texture Analyzer TAXT Plus (Stable Micro Systems Ltd., Surrey, UK) was used for the characterization of the bioadhesive profile of the developed formulations, using skin from fresh pig ears as biological model. The ears were obtained from a local slaughterhouse, following their preparation and set-up for the experiments according to previously published work [16, 17]. Prior the experiments, the skin ears were carefully cleaned with distilled water and frozen at -20.0 °C. For the experiment, nanoparticles were frozen at -80.0 °C for 24 h, and thendried in a freeze dryer during 48 h at 0.06 mbar (Labconco FreeZon®Freeze Dry Systems). During the analysis, the skin was kept in the lower platform of the texture analyzer, while the samples were fixed to the upper probe (10.0 mm of diameter) using double-side adhesive. Nanoparticles and skin were kept in close contact for 60 s at 32.0 ± 0.5 °C followed by the elevation of the probe at 0.5 mm/s. During the experiment, before the analysis, the biological samples were maintained in a physiological saline solution composed of NaCl 0.9% (w/v) in an ice bath. The bioadhesive properties of samples were expressed as tensile work (g.s), which has been obtained from the area under the force-time curve, as recommended [16]. For comparative analysis, Carbopol 971 hydrogel (C971) was used as reference due to its well-known mucoadhesive properties. All samples were analyzed in quintuplicate.

2.9. Texture profile analysis (TPA) of hydrogels

TPA analysis was carried out in a Texture Analyzer TAXT Plus (Stable Micro Systems Ltd., Surrey, UK) to evaluate the mechanical properties (hardness, adhesiveness and cohesiveness), as well as the springiness, gumminess, chewiness and resilience of the hydrogels. Hardness (g) was measured as the maximal stress reached during the first compression. The adhesiveness (g.s) was obtained as the area over the negative stress-strain curve after the first compression (work/volume). The cohesiveness was determined as the ratio of second compression and the first compression. Chewiness was calculated as the product of gumminess and springiness, which is the same as the product of hardness × cohesiveness × springiness. From the product of hardness × cohesiveness, gumminess was obtained. Springiness is a textural parameter related to the elasticity of the sample. Resilience was obtained as the ratio between energy released during recovery from deformation and the energy required for the deformation. Briefly, gels (10.0 g) were compressed uniaxially twice using an analytical probe at 1.0 mm/s to a predefined depth of 10.0 mm at a speed of 0.5 mm/s for each sample. The second compression was applied 5 s after the first one. Carbopol 971 gel (C971) was also used as gel reference for comparative analysis. All formulations were analysed in sextuplicate at 32.0 °C.

2.10. In-vitro Hen's egg test on the chorioallantoic membrane (HET-CAM)

To characterize the non-irritation profile of the hybrid nanoparticles before and after their dispersion into Carbopol hydrogels, the HET-CAM test has been performed as described before [18, 19, 20]. Eggs were firstly incubated at 38 ± 0.5 °C for a period of 10 days. The chorioallantoic membrane of the eggs was carefully removed using fine-tipped forceps to expose CAM. Parsol-SLN-Si were placed onto the embryonated hen's egg membrane, and the effects of nanoparticles monitored for 300 s. To characterize the semi-solid formulations (300 μL), these were firstly diluted in distilled water prior to their application onto the CAM of the eggs. As the positive control (for vascular hemorrhage and lysis), a volume of 300 μL of sodium hydroxide solution (0.1 M) was used. As the negative control, a volume of 300 μL of NaCl solution (0.9 wt.%) was used. The assays were performed in triplicate. Haemorrhage (H), lysis (L) and coagulation (C) were monitored over 300 s, recording the onset time of these three events. The standard irritation scores were calculated using the following equation:

$$300\ [IS] = 5\ [301 - H] + 7\ [301 - L] + 9\ [301 - C]$$

where IS stands for the irritation score, H for the onset time (in seconds) of bleeding, L for the onset time (in seconds) of lysis, C for the onset time (in seconds) of coagulation. The irritation profile was scored according to the following scale: from 0 to 0.9 as non-irritant; from 1 to 4.9 as slightly irritant; from 5 to 8.9 as moderately irritant; from 9 to 21 as strongly irritating.

2.11. Determination of the sun protection factor

The SPF of Parsol-SLN-Si was determined as described by Barbosa et al. [7], measured between 290 and 320 nm (UVB wavelength range), with increments of 5 nm. To estimate the SPF value of the developed formulation, Mansur et al. have proposed a mathematical model, applying the following equation [21]:

$$SPF_{spectrophotometric} = CF \times \sum_{290}^{320} EE_{(\lambda)} \times I_{(\lambda)} \times Abs_{(\lambda)}$$

in which CF stands for the correction factor, $EE_{(\lambda)}$ stands for the spectrum of erythemal effect, $I_{(\lambda)}$ for the spectrum of solar intensity and $Abs_{(\lambda)}$ for the sunscreen absorbance. As the $EE_{(\lambda)}$ and $I_{(\lambda)}$ are constant values, the SPF of the Parsol-SLN-Si could be estimated. Three determinations were made at each point.

2.12. Statistical analysis

All experiments were performed in triplicate, if not otherwise stated. A one-way analysis of variance (ANOVA) was used to analyse the statistical differences, considered significant for p-values below 0.05.

3. Results and discussion

The size parameters (mean particle size and PI) and zeta potential (PI) were compared among the three developed formulations when stored at room temperature over time. While blank SLN showed the lowest mean particle size and PI and higher ZP values, no statistically significant differences have been encountered for the three formulations (Table 2). On the day of the production, the loading of SLN with the sunscreen slightly increased the mean size and the PI (211.4 ± 1.085 nm and PI of 0.104 ± 0.111 for blank-SLN, and 243.1 ± 1.493 nm and PI of 0.300 ± 0.041 for Parsol-SLN). Freshly prepared Parsol-SLN resulted in the LC of 19.9% and EE of 98.3%, values attributed to the water-insolubility of the octyl methoxycinnamate thus with low partition into the water phase during the production of SLN [10]. High encapsulation parameters (LC and EE) are usually recorded for poorly water-soluble and lipophilic active ingredients

in lipid nanoparticles [22, 23]. The coating with silica improved the size parameters of Parsol-SLN (mean particle size of 210.0 ± 3.341 nm and PI < 0.300). Regardless the obtained mean particle size and polydispersity index, both non-coated and coated-particles could be used for topical application. Particles remain within a narrow size range over time. These results agree with previous reports, describing that the addition of silica-based polymers can shorten the distance between lipids and surfactants, leading to improved packing of nanoparticle surface and reduced particle size [24, 25]. Changes in the ZP values clearly indicate the presence of silica onto the surface of the particles. The particles can be stabilised in aqueous dispersion by different mechanisms, i.e. electrostatic (measured by ZP) and/or steric (hydrophilic chains of surfactants). The low zeta potential did not compromise the stability over time due to the presence of the emulsifying and reinforcement of the particle stability with the silica coating.

ZP was measured after diluting the original dispersion in water of conductivity previously adjusted to 50.0 μS/cm. Blank SLN showed the highest ZP values, although slightly negative, given the presence of the non-ionic emulsifier (Tego Care®450) onto the surface of the particles. The loading of SLN with Parsol did not significantly influence the ZP values, but the coating with TEOS decreased the surface electrical charge of the particles towards positive values after one month of storage at room temperature. These results confirm the successful development of hybrid nanoparticles. The literature reports that ZP values above |30| mV are preferential to achieve higher electrostatic stability of colloidal dispersions, |5| mV to |15| mV suggest of a range of limited flocculation while values between |3| mV to |5| mV the flocculation tends to a maximum [26, 27]. While exhibiting a slightly negative surface charge, the developed hybrid nanoparticles remained physicochemically stable over the study period.

Polymorphic transitions may occur within the lipid matrix of SLN, which may contribute to expel the drug from the carriers during storage. To tackle the risk of phase transitions, analysis of the crystallinity profile of SLN is needed which will also provide information on the loading capacity of the system for a specific drug and any potential interactions with excipients [28, 29]. The loading capacity of SLN decreases in the following sequence: supercooled melt, followed by the amorphous α-modification, the metastable β′-modification, and the most crystalline β-modification [30, 31]. The opposite happens with the lipid packing density and the thermodynamic stability. Figure 1 shows the thermograms of bulk cetyl palmitate, blank SLN, Parsol-SLN and Parsol-SLN coated with colloidal silica. The melting point of bulk cetyl palmitate was recorded between 56 °C and 57 °C, depicting a sharp peak. The onset temperature and enthalpy decreased with the use of the wax in SLN production, followed by the loading of particles with Parsol and the respective coating. These results translate a less organized lipid matrix mostly in the β′-modification, which contributes to maintain the drug loaded in the SLN [30, 32, 33].

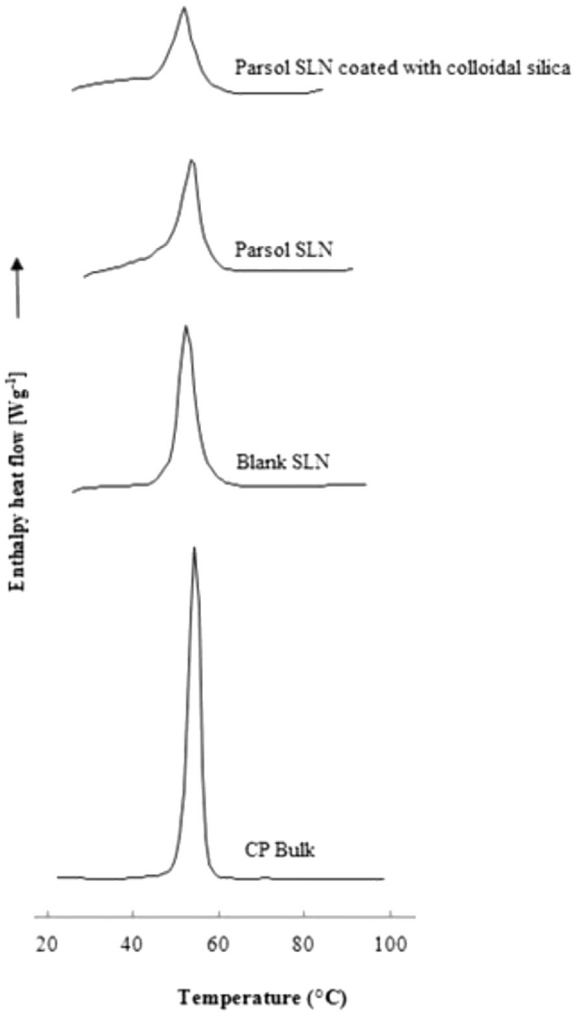

Figure 1. Thermograms of bulk cetyl palmitate, blank SLN, Parsol-SLN and Parsol-SLN coated with colloidal silica.

To confirm the long-term stability of the developed formulations, Turbiscan transmission profiles have been recorded. This type of measurement is based on the discrepancy of migration or coalescence of analyzed particles with further dissimilarity on the amount of light

Table 2. Particle size parameters and zeta potential of Blank SLN, Parsol-SLN and Parsol-SLN-Si at pre-determined time intervals for a period of 30 days.

Blank SLN	Z-Ave (nm) ± SD	PI ± SD	ZP (mV) ± SD
Day 0	211.4 ± 1.085	0.104 ± 0.111	-12.9 ± 0.331
Day 7	215.2 ± 2.014	0.163 ± 0.028	-11.4 ± 0.174
Day 15	222.5 ± 1.251	0.174 ± 0.031	-11.2 ± 0.531
Day 30	213.4 ± 1.932	0.179 ± 0.005	-10.3 ± 0.187
Parsol-SLN	Z-Ave (nm) ± SD	PI ± SD	ZP (mV) ± SD
Day 0	243.1 ± 1.493	0.300 ± 0.041	-9.6 ± 0.000
Day 7	248.4 ± 5.200	0.326 ± 0.044	-9.5 ± 0.119
Day 15	248.1 ± 2.173	0.361 ± 0.022	-8.5 ± 0.389
Day 30	248.0 ± 4.551	0.353 ± 0.011	-12.0 ± 0.236
Parsol-SLN-Si	Z-Ave (nm) ± SD	PI± SD	ZP (mV) ± SD
Day 0	210.0 ± 3.341	0.264 ± 0.009	-6.93 ± 0.745
Day 7	256.4 ± 5.369	0.396 ± 0.009	-5.19 ± 0.134
Day 15	214.3 ± 1.823	0.290 ± 0.026	-8.03 ± 0.435
Day 30	207.2 ± 5.595	0.287 ± 0.027	+4.02 ± 0.792

SD, standard deviation (n = 3 run; each run = 10 measurements); day = 0 stands for the day of production.

backscattered and transmitted [34, 35, 36]. Graphically, the light backscattered is presented as positive or negative variations *versus* time which is according to the pattern of particle migration. For example, if particles migrate in direction of the bottom of the assay tube, the concentration of those will increase at the center and bottom and decrease at the top [37]. As a result, the light will be less scattered at the top and more transmitted, resulting in a first negative peak with following expansion to positive values in consequence of growing concentrations of particles and thus increasing backscattered light.

In the present study, the samples were tested on a tube with the registry beginning from the bottom and a mark was made at a height of 20.0 mm. Three samples were employed from each formulation corresponding to separate times of measurement: at day 0, day 7 and day 15. For SLN, homogenous and almost without variation values for the three samples were registered; approximately from the very beginning of the tube measurement the backscattering light had a constant value of 80.0%, with differences noticeable only after the given mark (Figure 2 a). For Parsol-SLN an even softly beginning was seen with small loss values - 76.0%–80.0% of backscattered light - but homogenous although even after the 20.0 mm mark (Figure 2 b). For Parsol-SLN-Si the values were homogeneous, and the particles showed similar behavior, but overall values were slightly lower - about 70.0% of light scattering - below 20.0 mm mark. Above the given mark, the values fell down significantly. Such findings confirm the stability of the three tested formulations. Blank-SLN and Parsol-SLN showed improved colloidal stability over a period of 15 days after production.

The texture profile analysis of Parsol-SLN and Parsol-SLN-Si was carried out recording the adhesiveness, hardness, cohesiveness, springiness, gumminess, chewiness and the resilience (Table 3). For hardness parameter, Parsol-SLN-Si exhibited the lowest value, which was found better than Parsol-SLN as it represents the force needed to press the formulation until it offers the top resistance to compression [38]. Parsol-SLN-Si fitted better the desired profile for a topical application which requires a small force to spread the formulation onto the skin. Silica could apparently improve the texture properties for a topical application. With respect to adhesiveness, Parsol-SLN exhibited a higher value than Parsol-SLN-Si however attributed to the hardness parameter due to the apparent improved adhesiveness created by the highest pressure between the formulation and the base of the apparatus. Both formulations presented the same values for Springiness parameter revealing the same capacity to return to the initial design after deformation. Cohesiveness, which translates the product adhesiveness to itself or, in other terms, physical stability between molecules was almost the same for both formulations but Parsol-SLN-Si showed a slightly higher value. Both gumminess and chewiness were 1.5-fold higher in Parsol-SLN formulation, corroborating with the desired values observed for Parsol-SLN-Si formulation. The higher the hardness, the higher the gumminess and chewiness. Resilience parameter was almost the same for both formulations being slightly smaller for Parsol-SLN-Si which demonstrates a lower capacity against recovering the original height [39, 40, 41, 42].

Two different semi-solid formulations were produced by dispersing Parsol-SLN or Parsol-SLN-Si in Carbopol 917 hydrogels to achieve suitable viscosity for topical use. The bioadhesiveness of semi-solids were compared with the original dispersions and with a standard Carbopol 91 hydrogel (Table 4). Skin of pig ears has been used as ex-vivo model, following approval of the Ethics Committee (UNESP/Ethics Committee/Parsol-SLN/2015). Bioadhesiveness increased in the following order: C917 (6.69 g.s) < Parsol-SLN (7.13 g.s) < Parsol-SLN hydrogel (9.19 g.s) < Parsol-SLN-Si hydrogel (10.46 g.s) = Parsol-SLN-Si (10.46 g.s). Improved bioadhesiveness was achieved with the use of SLN in the hydrogels, which is in agreement with previous reports [39, 40]. Both Parsol-SLN-Si and Parsol-SLN-Si hydrogel had peak values for bioadhesiveness which put in evidence the role of SLN-silica combination as enhancer of this parameter in such a fashion that even an equal formulation but with inclusion in a hydrogel does not offer a better adhesiveness profile.

As the eye is more sensitive than healthy skin, and are commonly in contact with cosmetic and other UV blockers, the HET-CAM test has been run to measure the potential risk of irritation of Parsol-SLN-Si before and after their dispersion into hydrogels. This test consists on the determination of the risk of irritation by applying the formulation under study onto the chorion-allantoic membrane (CAM) of the chicken egg, and following determining hyperemia, hemorrhage, coagulation and lysis on the day 10 of the period of incubation [18, 19, 20]. It has been recently used as irritation test of sunscreen formulations [7]. No vascular events

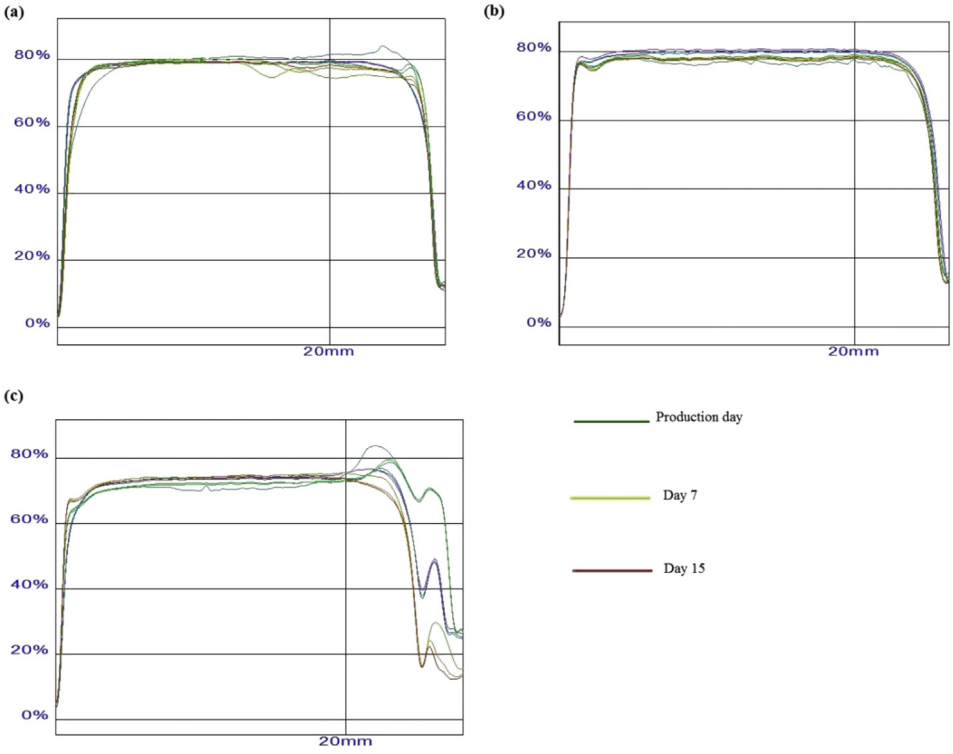

Figure 2. Turbiscan transmission profiles of (a) blank SLN, (b) Parsol-SLN and (c) Parsol-SLN coated with colloidal silica.

Table 3. Texture profile analysis (hardness (g), adhesiveness (g.s), springiness, cohesiveness, gumminess, chewiness and resilience) of Parsol-loaded SLN and Parsol-loaded SLN coated with silica gels (n = 3).

	Hardness	Adhesiveness	Springiness	Cohesiveness	Gumminess	Chewiness	Resilience
Parsol-SLN	6.52 ± 0.58	18.84 ± 4.39	0.85 ± 0.007	0.706 ± 0.021	1.62 ± 0.22	1.38 ± 0.18	0.18 ± 0.04
Parsol-SLN-Si	3.62 ± 0.13	11.55 ± 0.36	0.85 ± 0.01	0.74 ± 0.02	1.07 ± 0.05	0.91 ± 0.05	0.15 ± 0.01

Table 4. Bioadhesiveness (g.s) of Parsol-SLN and Parsol-SLN-Si before and after formulated in Carbopol C917 hydrogels in comparison to blank Carbopol C917 hydrogel.

Formulation	Bioadhesiveness (g.s)
C917	6.69 ± 0.64
Parsol-SLN	7.13 ± 2.28
Parsol-SLN hydrogel	9.19 ± 0.27
Parsol-SLN-Si hydrogel	10.46 ± 0.60
Parsol-SLN-Si	10.46 ± 0.51

were seen over the 300 s of the assay. The IS of 0.38 was recorded for the hydrogels containing particles, and of 0.39 for the Parsol-SLN-Si. Pure Carbopol hydrogels revealed an IS of 0.00.

According to the literature, concentration of 1% (w/w) of octyl methoxycinnamate (OMC) has been referred to offer an SPF of ca. 1.5. It is nevertheless expected that the loading of OMC into SLN increases the SPF by a synergistic effect, as SLN have already demonstrated scattering capacity. For the Parsol-SLN-Si, a SPF value of 10.62 has been obtained applying the Mansur equation. It is estimated that the scattering capacity of SLN could be reinforced by the coating with silica, which together with Parsol promoted the increasing of SPF. Similar results have been reported by Barbosa et al. who, upon loading poly-ϵ-caprolactone nanocapsules of SPF 6.84 with carrot oil, reached a SPF value of 8.64 [7]. Dutra et al. has shown that when combining octyl methoxycinnamate with other classical chemical or physical sunscreens (such as benzophenone-3, titanium dioxide, alkylbenzoate, octyl salicylate) in semi-solid formulations as emulsions the SPF can reach values above 15 [43]. Our developed semi-solid formulation, based on the dispersion of Parsol-SLN-Si in Carbopol hydrogels may further be improved with respect to its sun-blocking capacity by formulating additional sunscreens in the hydrogel.

4. Conclusions

Hybrid nanoparticles composed of lipids and silica have been proposed as a prominent delivery system for octyl methoxycinnamate. The loading of the sunscreen into cetyl palmitate-SLN has been confirmed by analysis of particle size parameters and by DSC. Particles remain physicochemically stable when stored at 25 °C over a period of 30 days. The coating of particles with colloidal silica contributed for the improvement of bioadhesiveness of the developed hydrogels. Hydrogels exhibited properties for topical administration and did not induce irritation effects on the HET-CAM. Further studies are planned to further evaluate the effect on the bioadhesion with increasing concentration of hybrid nanoparticles, in comparison to plain hydrogels, to explore the bioadhesion cumulative effect after adding non-coated and silica-coated SLN. The synergistic effect of the loading of Parsol into SLN in the increase of the SPF has also been demonstrated.

Declarations

Author contribution statement

Eliana B. Souto: Conceived and designed the experiments; Analyzed and interpreted the data; Contributed reagents, materials, analysis tools or data; Wrote the paper.

Tatiana Andreani: Conceived and designed the experiments; Performed the experiments; Analyzed and interpreted the data; Wrote the paper.

João Ferreira: Performed the experiments; Analyzed and interpreted the data; Wrote the paper.

Joana F. Fangueiro, Ana Luiza Ribeiro de Souza, Charlene Kiill, Maria Palmira Gremiao: Performed the experiments; Analyzed and interpreted the data.

Amelia Silva: Conceived and designed the experiments; Analyzed and interpreted the data; Contributed reagents, materials, analysis tools or data.

Maria Luisa Garcia: Analyzed and interpreted the data; Contributed reagents, materials, analysis tools or data.

Funding statement

This work was supported by the Portuguese Science and Technology Foundation (FCT/MCT) and European Funds (PRODER/COMPETE), co-financed by FEDER, under the Partnership Agreement PT2020 through the projects M-ERA-NET/0004/2015-PAIRED and UIDB/04469/2020 (granted to Eliana B. Souto) and UID/AGR/04033/2019 (granted to Amélia M. Silva).

Competing interest statement

The authors declare no conflict of interest.

Additional information

No additional information is available for this paper.

References

[1] D.R. Sambandan, D. Ratner, Sunscreens: an overview and update, J. Am. Acad. Dermatol. 64 (2011) 748–758.
[2] N. Serpone, D. Dondi, A. Albini, Inorganic and organic UV filters: their role and efficacy in sunscreens and suncare products, Inorg. Chim. Acta. 360 (2007) 794–802.
[3] J.A. Ruszkiewicz, A. Pinkas, B. Ferrer, T.V. Peres, A. Tsatsakis, M. Aschner, Neurotoxic effect of active ingredients in sunscreen products, a contemporary review, Toxicol. Rep. 4 (2017) 245–259.
[4] M. Krause, A. Klit, M.B. Jensen, T. Søeborg, H. Frederiksen, M. Schlumpf, W. Lichtensteiger, N.E. Skakkebaek, K.T. Drzewiecki, Sunscreens: are they beneficial for health? An overview of endocrine disrupting properties of UV-filters, Int. J. Androl. 35 (2012) 424–436.
[5] E.B. Souto, C. Anselmi, M. Centini, R.H. Muller, Preparation and characterization of n-dodecyl-ferulate-loaded solid lipid nanoparticles (SLN), Int. J. Pharm. 295 (2005) 261–268.
[6] Q. Xia, A. Saupe, R.H. Muller, E.B. Souto, Nanostructured lipid carriers as novel carrier for sunscreen formulations, Int. J. Cosmet. Sci. 29 (2007) 473–482.
[7] T.C. Barbosa, L.E.D. Nascimento, C. Bani, T. Almeida, M. Nery, R.S. Santos, L.R.O. Menezes, A. Zielinska, A.R. Fernandes, J.C. Cardoso, A. Jaguer, E. Jaguer, E. Sanchez-Lopez, L. Nalone, E.B. Souto, P. Severino, Development, Cytotoxicity and eye irritation profile of a new sunscreen formulation based on benzophenone-3-poly(epsilon-caprolactone) nanocapsules, Toxics 7 (2019).
[8] A. Lohani, A. Verma, H. Joshi, N. Yadav, N. Karki, Nanotechnology-based cosmeceuticals, ISRN Dermatol. 2014 (2014) 843687.
[9] P.K. Indu, A. Rumjhum, Nanotechnology: a new paradigm in cosmeceuticals, Recent Pat. Drug Deliv. Formulation 1 (2007) 171–182.
[10] E.B. Souto, I. Baldim, W.P. Oliveira, R. Rao, N. Yadav, F.M. Gama, S. Mahant, SLN and NLC for topical, dermal and transdermal drug delivery, Expet Opin. Drug Deliv. 17 (2020) 357–377.
[11] S.H. Tolbert, P.D. McFadden, D.A. Loy, New hybrid organic/inorganic polysilsesquioxane-silica particles as sunscreens, ACS Appl. Mater. Interfaces 8 (2016) 3160–3174.

[12] N. Koike, T. Ikuno, T. Okubo, A. Shimojima, Synthesis of monodisperse organosilica nanoparticles with hollow interiors and porous shells using silica nanospheres as templates, Chem. Commun. (Camb) 49 (2013) 4998–5000.
[13] L.B. Lopes, Overcoming the cutaneous barrier with microemulsions, Pharmaceutics 6 (2014) 52–77.
[14] M.E. Carlotti, M. Gallarate, V. Rossatto, O/W microemulsion as a vehicle for sunscreens, J. Cosmet. Sci. 54 (2003) 451–462.
[15] E.B. Souto, S. Doktorovova, A. Zielinska, A.M. Silva, Key production parameters for the development of solid lipid nanoparticles by high shear homogenization, Pharmaceut. Dev. Technol. 24 (2019) 1181–1185.
[16] S. Barbi Mda, F.C. Carvalho, C.P. Kiill, S. Barud Hda, S.H. Santagneli, S.J. Ribeiro, M.P. Gremiao, Preparation and characterization of chitosan nanoparticles for zidovudine nasal delivery, J. Nanosci. Nanotechnol. 15 (2015) 865–874.
[17] A.L. Ruela, F.C. Carvalho, G.R. Pereira, Exploring the phase behavior of monoolein/oleic acid/water systems for enhanced donezepil administration for Alzheimer disease treatment, J. Pharmacol. Sci. 105 (2016) 71–77.
[18] E. Sanchez-Lopez, M.A. Egea, A. Cano, M. Espina, A.C. Calpena, M. Ettcheto, A. Camins, E.B. Souto, A.M. Silva, M.L. Garcia, PEGylated PLGA nanospheres optimized by design of experiments for ocular administration of dexibuprofen-in vitro, ex vivo and in vivo characterization, Colloids Surf. B Biointerfaces 145 (2016) 241–250.
[19] J.F. Fangueiro, A.C. Calpena, B. Clares, T. Andreani, M.A. Egea, F.J. Veiga, M.L. Garcia, A.M. Silva, E.B. Souto, Biopharmaceutical evaluation of epigallocatechin gallate-loaded cationic lipid nanoparticles (EGCG-LNs): in vivo, in vitro and ex vivo studies, Int. J. Pharm. 502 (2016) 161–169.
[20] J. Araujo, E. Vega, C. Lopes, M.A. Egea, M.L. Garcia, E.B. Souto, Effect of polymer viscosity on physicochemical properties and ocular tolerance of FB-loaded PLGA nanospheres, Colloids Surf. B Biointerfaces 72 (2009) 48–56.
[21] J.S. Mansur, M.N.R. Breder, M.C.A. Mansur, R.D. Azulay, Determinação do fator de proteção solar por espectrofotometria, An. Bras. Dermatol. 61 (1986) 121–124.
[22] E.B. Souto, S.B. Souto, A. Zielinska, A. Durazzo, M. Lucarini, A. Santini, O.K. Horbańczuk, A.G. Atanasov, C. Marques, L.N. Andrade, A.M. Silva, P. Severino, Perillaldehyde 1,2-epoxide loaded SLN-tailored mAb: production, physicochemical characterization and in vitro cytotoxicity profile in MCF-7 cell lines, Pharmaceutics 12 (2020) 161.
[23] E.B. Souto, A. Zielinska, S.B. Souto, A. Durazzo, M. Lucarini, A. Santini, A.M. Silva, A.G. Atanasov, C. Marques, L.N. Andrade, P. Severino, (+)-Limonene 1,2-epoxide-loaded SLN: evaluation of drug release, antioxidant activity and cytotoxicity in HaCaT cell line, Int. J. Mol. Sci. 21 (2020) E1449.
[24] J. Shaji, D. Varkey, Silica-coated solid lipid nanoparticles enhance antioxidant and antiradical effects of meloxicam, J. Pharmaceut. Invest. 43 (2013) 405–416.
[25] S. Kim, R. Diab, O. Joubert, N. Canilho, A. Pasc, Core-shell microcapsules of solid lipid nanoparticles and mesoporous silica for enhanced oral delivery of curcumin, Colloids Surf. B Biointerfaces 140 (2016) 161–168.
[26] R.H. Muller, K. Mader, S. Gohla, Solid lipid nanoparticles (SLN) for controlled drug delivery - a review of the state of the art, Eur. J. Pharm. Biopharm. 50 (2000) 161–177.
[27] Z. Rahman, A.S. Zidan, M.J. Habib, M.A. Khan, Understanding the quality of protein loaded PLGA nanoparticles variability by Plackett–Burman design, Int. J. Pharm. 389 (2010) 186–194.
[28] P. Severino, S.C. Pinho, E.B. Souto, M.H. Santana, Polymorphism, crystallinity and hydrophilic-lipophilic balance of stearic acid and stearic acid-capric/caprylic triglyceride matrices for production of stable nanoparticles, Colloids Surf. B Biointerfaces 86 (2011) 125–130.
[29] M. Cavendish, L. Nalone, T. Barbosa, R. Barbosa, S. Costa, R. Nunes, C.F. da Silva, M.V. Chaud, E.B. Souto, L. Hollanda, P. Severino, Study of pre-formulation and development of solid lipid nanoparticles containing perillyl alcohol, J. Therm. Anal. Calorim. (2019) 1–8.
[30] E.B. Souto, W. Mehnert, R.H. Muller, Polymorphic behaviour of Compritol888 ATO as bulk lipid and as SLN and NLC, J. Microencapsul. 23 (2006) 417–433.
[31] E.B. Souto, R.H. Muller, Lipid nanoparticles: effect on bioavailability and pharmacokinetic changes, Handb. Exp. Pharmacol. (2010) 115–141.
[32] E.B. Souto, R.H. Muller, Investigation of the factors influencing the incorporation of clotrimazole in SLN and NLC prepared by hot high-pressure homogenization, J. Microencapsul. 23 (2006) 377–388.
[33] E. Zimmermann, E.B. Souto, R.H. Muller, Physicochemical investigations on the structure of drug-free and drug-loaded solid lipid nanoparticles (SLN) by means of DSC and 1H NMR, Pharmazie 60 (2005) 508–513.
[34] A. Zielinska, N.R. Ferreira, A. Durazzo, M. Lucarini, N. Cicero, S.E. Mamouni, A.M. Silva, I. Nowak, A. Santini, E.B. Souto, Development and optimization of alpha-pinene-loaded solid lipid nanoparticles (SLN) using experimental factorial design and dispersion analysis, Molecules 24 (2019).
[35] A. Zielinska, C. Martins-Gomes, N.R. Ferreira, A.M. Silva, I. Nowak, E.B. Souto, Anti-inflammatory and anti-cancer activity of citral: optimization of citral-loaded solid lipid nanoparticles (SLN) using experimental factorial design and LUMiSizer(R), Int. J. Pharm. 553 (2018) 428–440.
[36] A. Zielińska, N.R. Ferreira, A. Feliczak-Guzik, I. Nowak, E.B. Souto, Loading, release profile and accelerated stability assessment of monoterpenes-loaded Solid Lipid Nanoparticles (SLN), Pharmaceut. Dev. Technol. (2020).
[37] C. Celia, E. Trapasso, D. Cosco, D. Paolino, M. Fresta, Turbiscan lab expert analysis of the stability of ethosomes and ultradeformable liposomes containing a bilayer fluidizing agent, Colloids Surf. B Biointerfaces 72 (2009) 155–160.
[38] L.C. Cefali, J.A. Ataide, S. Eberlin, F.C. da Silva Goncalves, A.R. Fernandes, J. Marto, H.M. Ribeiro, M.A. Foglio, P.G. Mazzola, E.B. Souto, In vitro SPF and photostability assays of emulsion containing nanoparticles with vegetable extracts rich in flavonoids, AAPS PharmSciTech 20 (2018) 9.
[39] E.B. Souto, R.H. Muller, Rheological and in vitro release behaviour of clotrimazole-containing aqueous SLN dispersions and commercial creams, Pharmazie 62 (2007) 505–509.
[40] E.B. Souto, S.A. Wissing, C.M. Barbosa, R.H. Muller, Evaluation of the physical stability of SLN and NLC before and after incorporation into hydrogel formulations, Eur. J. Pharm. Biopharm. 58 (2004) 83–90.
[41] E.B. Souto, R.H. Muller, The use of SLN and NLC as topical particulate carriers for imidazole antifungal agents, Pharmazie 61 (2006) 431–437.
[42] E.B. Souto, S.H. Gohla, R.H. Muller, Rheology of nanostructured lipid carriers (NLC) suspended in a viscoelastic medium, Pharmazie 60 (2005) 671–673.
[43] E.A. Dutra, D.A.G.C. Oliveira, E.R.M. Kedor-Hackmann, M.I.R.M. Santoro, Determination of sun protection factor (SPF) of sunscreens by ultraviolet spectrophotometry, Rev. Bras. Ciencias Farm. 40 (2004) 381–385.